Available online at www.sciencedirect.com
SCIENCE DIRECT
Journal of Photochemistry and Photobiology A: Chemistry 175 (2005) 8–14
Journal of Photochemistry and Photobiology A:Chemistry
www.elsevier.com/locate/jphotochem

Femtosecond to nanosecond spectroscopy of transition metal-doped TiO_2 particles

Miia Salmi [a,*], Nikolai Tkachenko [a], Ralf-Johan Lamminmäki [b], Saila Karvinen [b], Visa Vehmanen [b], Helge Lemmetyinen [a]

[a] *Institute of Materials Chemistry, Tampere University of Technology, P.O. Box 541, FIN-33101 Tampere, Finland*
[b] *Kemira Pigments Oy, FIN-28840 Pori, Finland*

Received 31 August 2004; received in revised form 17 March 2005; accepted 29 March 2005
Available online 22 April 2005

Abstract

The transient absorption properties of TiO_2 particles were studied by femtosecond transient absorption spectroscopy. For the transition metal (Cr and/or Fe)-doped samples the transient absorption spectra were observed to shift to the shorter wavelengths with the time while for the non-doped sample the position of the absorptions did not change. The spectral shifts were the highest for the sample doped by both Cr and Fe. The transient absorption spectra right after excitation had a broad absorption band with the flat top in 550–650 nm region, whereas at 1 ns delay the maximum of the transient absorption shifted to 510–530 nm area for Cr- and Fe-doped samples. The observed new absorption bands were attributed to the trapped holes. For comparison, activity measurements for the same samples were performed in photocatalytic reactor system. Doping reduced the photocatalytic activity of the samples. This can be interpreted in favour of the importance of the hot and shallow trapped holes for the photocatalytic activity, which gains another relaxation channel of trapping by the doping transition metals.
Published by Elsevier B.V.

Keywords: TiO_2; Photocatalysis; Femtosecond spectroscopy; Doping

1. Introduction

The use of TiO_2 as a photocatalyst has been widely studied in the past decades and a lot of research has been done for the development of highly active photocatalytic materials [1–5]. TiO_2 has relatively large band-gap energy and thus it utilizes only a small fraction of the solar spectrum. For anatase the band-gap energy is $E_{bg} = 3.23$ eV and for rutile $E_{bg} = 3.00$ eV [6], thus the wavelengths shorter than 380 and 410 nm are needed for the excitation. To extend the photoresponse into the visible part of the spectrum a doping of TiO_2 with transition metals have been employed [7]. Metal ions can also serve as charge trapping sites and thus reduce electron–hole recombination rate [8,9]. The effect of doping on the activity depends on many factors, e.g. the method of doping, and the type and the concentration of a dopant [7]. Both detrimental and enhancive effects of transition metal ion doping have been reported [7,10–16]. The comparison between the reported results is difficult since in addition to different preparation methods of the doped samples, the experimental conditions for the determination of photoreactivity have been varying.

Charge carrier dynamics are one of the important factors affecting the photocatalytic activity of the TiO_2 particles. Only few reports, however, have been published concerning the effect of doping on charge carrier dynamics [10,11,17]. Choi et al. [10] studied the role of metal ion dopants on charge carrier recombination in TiO_2 colloids by flash photolysis spectroscopy. Type of the dopant and its concentration were reported to affect the transient absorption signals, which were attributed to the trapped electrons. The photocatalytic activity of the doped samples was observed to correlate with the amount of the photogenerated charge carriers that survived recombination over the nano- to microsecond time domain. The transient absorption signals upon laser flash photolysis

* Corresponding author. Tel.: +358 3 31152631; fax: +358 3 31152108.
E-mail address: miia.salmi@tut.fi (M. Salmi).

1010-6030/$ – see front matter. Published by Elsevier B.V.
doi:10.1016/j.jphotochem.2005.03.022

were extended up to 50 ms for Fe^{3+}-, V^{4+}-, Mo^{5+}- and Ru^{3+}-doped TiO_2 while the non-doped and Co^{3+}- and Al^{3+}-doped TiO_2 had signal decays in microsecond timescale. Ikeda et al. [11] have employed femtosecond pump-probe diffuse reflectance spectroscopy to study photoresponses at 620 nm of TiO_2 powders doped with various transition metals (V, Cr, Fe, Co, Cu, Mo and W). The signals were fitted to the second order kinetics and the rates were considered to represent the recombination rates of the photogenerated electrons and holes. The recombination rates of the doped samples were shown to be faster than that of the non-doped sample and to increase with the amount of the dopant. The observed recombination rates were also compared to the measured photocatalytic activities for the degradation of some model compounds and the correlation was found between the low recombination rate and the high photocatalytic activity. Furube et al. [17] have measured transient absorption spectra of Pt-loaded TiO_2 powder and were able to show the migration of electrons in TiO_2 to Pt in few picoseconds.

The aim of the present work is to study the effect of the doping on charge carrier dynamics of TiO_2 particles by doping it by Cr or Fe or both Cr and Fe. This was fulfilled employing femtosecond absorption pump-probe spectroscopy and thus obtaining information on primary femto–picosecond carrier relaxation processes. To our knowledge this is the first report on doping effect of Fe and Cr carried out in a wide spectrum range in the femtosecond time domain. In addition, the photocatalytic activity of the same samples was studied in a photocatalytic reactor system using acetaldehyde and toluene as model compounds. The relation of the time-resolved spectroscopic results to the nature and the photocatalytic activity of the particles is discussed.

2. Experimental

2.1. Samples

TiO_2 nanocrystalline anatase powder samples doped by Cr, Fe or both Cr and Fe were supplied by Kemira Pigments Oy (Pori, Finland). The samples were precipitated from $TiOSO_4$ solution according to the previously described method (series A) [18] and doped by the wet-impregnation method. Two doping concentrations were used, 0.2 and 0.4%. However, the results were virtually the same for these concentrations, therefore only data obtained for 0.2% samples are

Table 1
The physical properties of the TiO_2 powder samples

Sample	Specific surface area[a] ($m^2\,g^{-1}$)	Content of Cr[b] ($mg\,kg^{-1}$)	Content of Fe[b] ($mg\,kg^{-1}$)
TiO_2	207	6	<25
TiO_2/Cr	228	2100	<25
TiO_2/Fe	192	7	2100
TiO_2/Cr–Fe	221	2100	2100

[a] Measured by the BET method (N_2 as adsorbate) using a Quantachrome Monosorb apparatus.
[b] Measured by graphite furnace atomic absorption spectrofotometry (GFAAS).

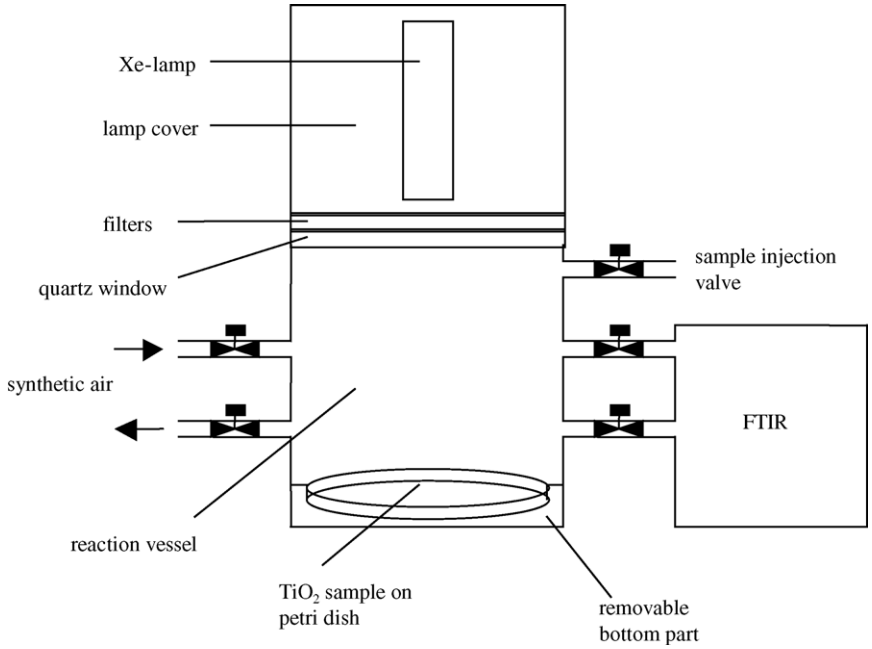

Fig. 1. Schematic diagram of a flow-type reactor employed to carry out the photocatalytic degradation of gaseous acetaldehyde and toluene.

reported in this paper. The physical properties of the samples are presented in Table 1.

For the spectroscopic measurements the TiO_2 films were prepared on glass substrates by mixing 400 mg TiO_2 powder with 1 ml 1-butanol, spreading resulting particle suspension onto the glass substrate and smoothing it with a glass rod using adhesive tape as a border. The films were dried in air.

2.2. Spectroscopic study

Absorption spectra of the TiO_2 films were recorded on a Shimadzu UV-2501PC. Femtosecond to picosecond time-resolved absorption spectra were measured using the pump-probe technique. The set-up is reported elsewhere [19]. The excitation wavelength was 390 nm (second harmonic of the Ti:sapphire laser) and the spectra were recorded in the wavelength range 460–680 nm using white-light continuum. Time resolution of the instrument was about 300 fs (FWHM).

2.3. Photocatalytic reactor experiments

The photocatalytic degradation of acetaldehyde and toluene was analysed using a flow-type reactor as schematically shown in Fig. 1. The irradiation source was 300 W Xe-lamp (Thermo Oriel Instruments, Stratford, USA). A filter was used to cut off the wavelengths below 385 nm. The experiments were started by opening the removable bottom part and adjusting the water level in the reactor to $10\,000 \pm 1000$ ppm. The sample in a Petri dish was placed in the bottom part of the reactor and the system was closed. One microliter 25% acetaldehyde–water mixture and 0.2 μl toluene were injected through the sample injection valve to the reactor. The system was allowed to stabilize for few minutes and then illuminated. The irradiated system was continuously running through the reactor vessel and FT-IR spectrophotometer at a flow rate of 25 ml s^{-1}. The system was programmed to monitor the concentrations of water (monitoring wavelength range 3200–3401 cm^{-1}), carbon dioxide (2200–2350 cm^{-1}), carbon monoxide (2030–2200 cm^{-1}), acetaldehyde (2609–2918 cm^{-1}) and toluene (2950–3149 cm^{-1}). After each experiment the system was flushed by synthetic air.

3. Results and discussion

3.1. Steady-state absorption

The absorption spectra of the prepared films of the samples are shown in Fig. 2.

The spectra were measured for two reasons: to control the quality of the films and to determine the absorption edges of the samples. The absorption is at the level of about 2.5 at the wavelength area from 400/500 nm to 800 nm. TiO_2 does not absorb at these wavelengths, thus the high "background absorption" is due to scattering and reflection of the light from the semi-transparent samples. As the absorption level is about the same at 800 nm for all the samples one can conclude that the thicknesses of the films are roughly the same. Doping with Fe seems not to have any considerable effect on the absorption because both the non-doped sample and the Fe-doped sample show absorptions typical to anatase particles (band edge at 384 nm) [6]. Doping with chromium causes the absorption to shift towards the visible region and the absorption band edge starts at about 500 nm. The absorption spectra of the samples doped by Cr or both Cr and Fe were identical, thus Fe dopants did not affect the absorption in the latter case as well. Due to the high scattering property of the samples a small spectrum difference between the different samples cannot be observed and the actual shape of the absorptions cannot be concluded. The spectra could be measured in the reflectance mode but this method was unavailable for the study.

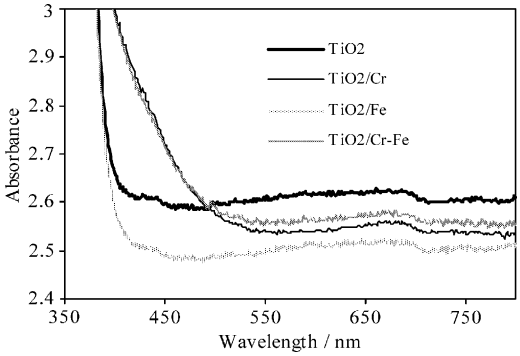

Fig. 2. Absorption spectra of the doped and non-doped TiO_2 powder samples measured on films.

3.2. Transient absorptions of TiO_2 films

Transient absorption signals of the TiO_2 films were recorded at the wavelength range 460–680 nm and were used to generate transient absorption decay curves in the same range. Multiexponential global fittings were applied to the transient absorption decay curves at different wavelengths [19]:

$$D(t, \lambda) = a_0(\lambda) + \sum a_i(\lambda) \exp(-t/\tau_i) \quad (1)$$

where τ_i represent the lifetimes and $a_i(\lambda)$ the corresponding pre-exponential factors. The fitting program has also accounted for the instrument response function (using deconvolution routine), and the group velocity dispersion. This extended the time resolution of the system and allowed us to calculate dispersion compensated spectra at short delay times.

Three-exponential fittings gave reasonably good results for all the samples. The obtained transient absorption component spectra for the non-doped and doped samples are shown in Fig. 3A, C, E and G. The differential time-resolved spectra at delay times $t = 0$ ps, 5 ps and 1 ns were calculated using Eq. (1) and are shown in Fig. 3B, D, F and H.

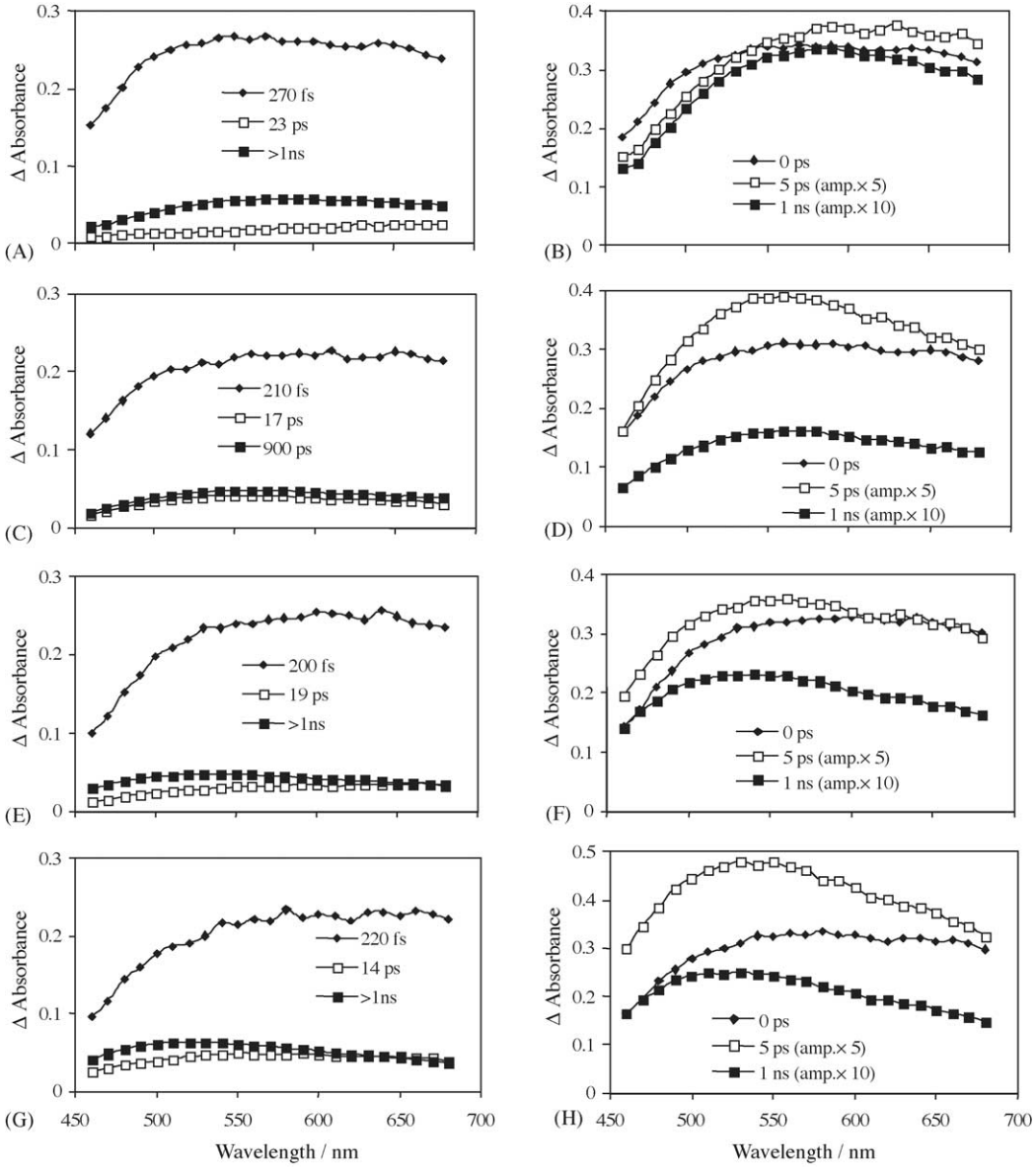

Fig. 3. Transient absorption component spectra of TiO_2 films (A, C, E and G) and differential time-resolved spectra at $t = 0$, 5 ps and 1 ns (B, D, F and H): (A, B) TiO_2; (C, D) TiO_2/Cr; (E, F) TiO_2/Fe; (G, H) TiO_2/Cr–Fe. The intensities of the spectra at $t = 5$ ps and 1 ns are multiplied by 5 and 10 (B, D, F and H), respectively. Lifetimes of the components are indicated (A, C, E and G).

For all the samples a fast decay (200–300 fs), a picosecond relaxation (14–25 ps) and a long-lived component (>1 ns) were observed. The fast decay component was at the limit of the instrument time resolution, and comparison of the decay time constants is hardly possible. However, this was dominating component for all the samples and de-convolution fit procedure tend to account for as fast as 100 fs relaxation. Therefore, the spectrum calculated for $t = 0$ ps delay should give a reasonable figure for the processes which are slower than 100 fs. Noticeably, the spectra calculated for $t = 0$ ps delay (Fig. 3B, D, F and H) are virtually identical for all the samples, whereas at longer delay times a considerable difference in the shape and amplitude of the spectra can be seen.

3.3. Character of photogenerated charge carriers

The trapping of the conduction band electrons and valence band holes at shallow or deep trapping sites are reported to occur in less than few hundred femtoseconds and the observed transient absorption immediately after the excitation is generally attributed to the charge carriers electrons and/or holes already trapped to different energy states [20,21]. The fast relaxation observed for the studied samples is in agreement with the previous observations of the trapping dynamics of hot and shallow trapped carriers. Therefore, the transient absorption spectrum at $t = 0$ ps can be attributed to hot and/or shallow carriers. Although the limit in time resolution does not allow us to distinguish between the hot and shallow traps,

the spectra at $t = 0$ ps are virtually identical for all the samples which indicates that at very short delay time the doping of the samples has no yet effect. However, after fast relaxation (<300 fs), when the carriers are trapped at deeper trapping sites, the spectra of the samples have clearly different shapes. This is apparently due to the doping effect, and can be analysed considering the change in the shape of the transient absorption spectra.

In the nanosecond flash photolysis experiments, the transient absorption spectra of the trapped holes and electrons has been observed through hole- or electron-scavenging reactions [22,23]. The maximum absorption has been observed for the trapped holes as a broad band in the blue part of the spectrum at 475 nm [22] or 520 nm [23] and for the trapped electrons in the red part of the spectrum at 650 nm [22] or 770 nm [23] depending the experimental conditions. In the femtosecond transient absorption spectroscopy experiments, an absorption band around 520 nm was observed immediately after the band-gap excitation for the nanosized anatase TiO_2 colloidal particles and it was regarded as an absorption of shallowly trapped holes [21]. In this study, the shapes of the spectra for the non-doped and doped samples were different. In order to see the differences in the shapes of the transient absorption spectra normalized spectra (intensity at 680 nm adjusted to 1) of different samples at certain times are presented one upon the other in Fig. 4.

At $t = 0$ ps the shapes of the spectra of all the samples are practically identical (Fig. 4A). Also the intensities of the spectra at $t = 0$ ps are about the same for all the samples (Fig. 3). The absorption is higher at long wavelength area than at short wavelength area but no distinct absorption bands are observed. Compared to the spectra presented in the literature for the trapped electrons and trapped holes the first intermediate state is attributed to the absorption of electrons or both the electrons and holes (hot or shallowly trapped).

At $t = 5$ ps and 1 ns clear differences are observed between the transient absorption spectra of the different samples (Fig. 4B and C). The absorption of the non-doped sample stays the same during the measured time range while the absorption maxima of the spectra of the doped samples shift to the shorter wavelengths with time. At $t = 5$ ps the absorption maxima of the Cr- and Fe-doped samples are at 560 nm and the absorption maximum of the Cr–Fe-doped sample is at 530 nm (Fig. 4B and C). The absorption of the Cr-doped sample stays the same during the time range from 5 ps to 1 ns, whereas for the Fe- and Fe–Cr-doped samples the absorption still shifts to shorter wavelengths and at $t = 1$ ns they are at 540 and 520 nm, respectively (Fig. 4C). The absorption maximum at 520 nm corresponds to the absorption maximum of the trapped holes [22,23]. Thus, the spectral shift of the absorption to shorter wavelengths is considered to be due to the existence of relatively larger amount of the trapped holes compared to the trapped electrons at timescales longer than 0.3 ps.

The relative amplitudes of the spectra at different delay times are different for the different samples. To compare the

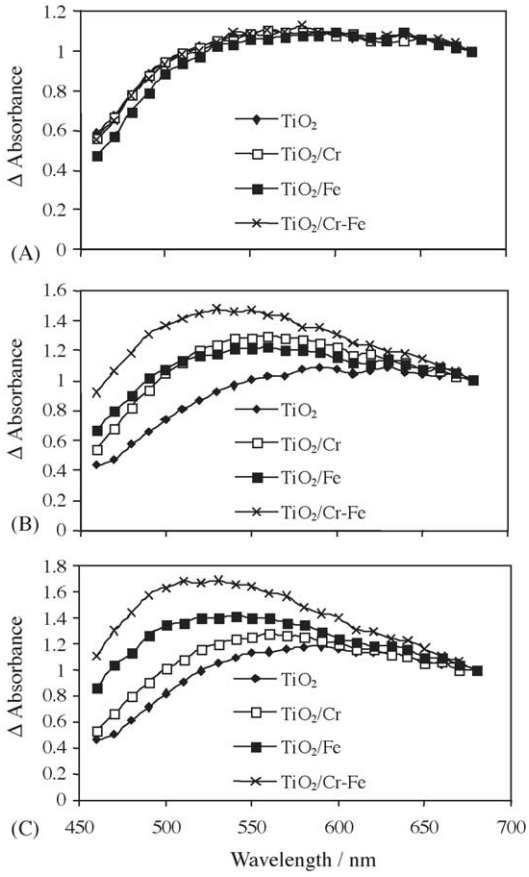

Fig. 4. Normalized (at 680 nm) transient absorption spectra of the studied TiO_2 powder films at $t = 0$ ps (A), $t = 5$ ps (B) and $t = 1$ ns (C).

relative intensities of the components the normalized transient absorption decay curves of the samples at the monitoring wavelengths 480 and 680 nm are shown in Fig. 5. At the monitoring wavelength 680 nm the decay curves are the same for all the samples. According to literature the absorption at this wavelength represent mainly the absorption of the trapped electrons [22,23]. At the monitoring wavelength 480 nm differences are observed between the particles doped by different metals. The absorption at this wavelength depicts (in addition of the absorption of the trapped electrons) the absorption of the trapped holes. The order of the increase in the relative amplitudes of the absorptions after the initial fast decay at 480 nm were found to be TiO_2/Cr–Fe > TiO_2/Fe > TiO_2/Cr > TiO_2. Thus, it seems that relatively larger amounts of the trapped holes are formed for the doped particles as already was concluded based on the shapes of the spectra (Fig. 4). For the iron-doped TiO_2 particles trapping of both the electrons and the holes at Fe^{3+} sites has been reported previously [9]. Trapping of the holes at Cr^{3+} sites has been proposed for the chromium-doped TiO_2 samples [24]. Since the observed absorption for the Fe- and Cr–Fe-doped samples at $t = 1$ ns corresponds to the absorption reported in the literature for the trapped holes, we propose that it is caused by the trapping of the electrons by Fe (and probably also by Cr in latter) which reduces the electron–hole re-

Table 2
Rate constants of TiO_2 powder samples for acetaldehyde and toluene degradation

Sample	CO_2		Acetaldehyde		Toluene	
	k^a ($\times 10^{-10}$ mol dm^{-3} s^{-1})	R	k^b ($\times 10^{-4}$ s^{-1})	R	k^b ($\times 10^{-4}$ s^{-1})	R
TiO_2	5.59	0.99	3.88	1.00	5.27	1.00
TiO_2/Cr	0.36	0.99	0.23	0.82	0.42	1.00
TiO_2/Fe	2.21	0.97	1.42	1.00	2.04	1.00
TiO_2/Cr–Fe	0.68	0.79	0.83	0.96	0.47	1.00

[a] Zero-order rate constant.
[b] First-order rate constant.

combination. The trapping of the electrons by Cr can explain the shift in the absorption in the Cr-doped samples though the observed shift is not large. In the research of Ikeda et al. [11] the charge carrier dynamics of various doped TiO_2 samples were studied by observing the transient absorption at 620 nm. At this wavelength the decays were attributed to the recombination of electrons and holes. In the present study at a wide spectrum range we have shown that the transient absorption decays of the doped samples are more complex functions of the trapping and the recombination of electrons and/or holes. Doping introduces some imbalance in the electron–hole recombination as compared to the non-doped particles.

3.4. Degradation of acetaldehyde and toluene

A comparison of the photocatalytic activities of the samples was conducted by degrading acetaldehyde–toluene mixture in a photocatalytic reactor system. The disappearances of acetaldehyde and toluene and the generation of CO_2 were monitored as a function of time of irradiation. The results of the acetaldehyde and toluene degradations were fitted to the first order kinetics and the formation of CO_2 to the zero order kinetics. The rate constants and the correlation coefficients of the fittings are presented in Table 2.

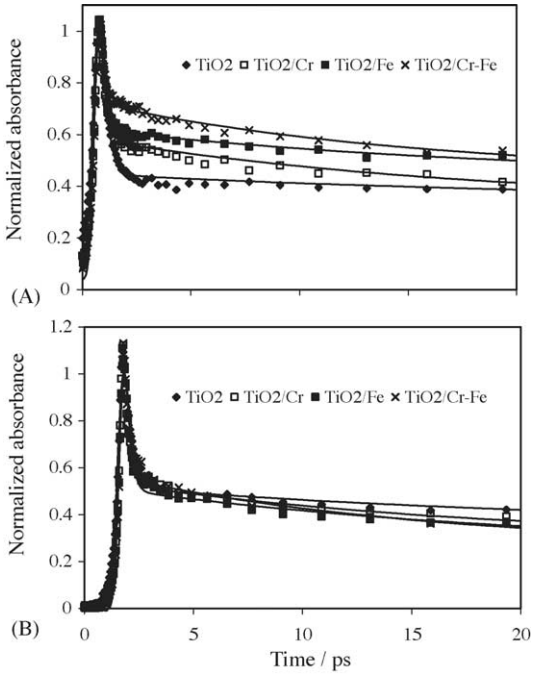

Fig. 5. Normalized transient absorption decay curves of non-doped and metal-doped TiO_2 powders at monitoring wavelengths 480 nm (A) and 680 nm (B).

It can be seen from Table 2 that the doping reduces the activity. The activity decreased in the order $TiO_2 > TiO_2$/Fe > TiO_2/Cr–Fe > TiO_2/Cr. The doping of the samples by Cr or Cr and Fe eliminates the activity of the samples almost totally while some activity was remained after doping with iron. Comparing this with the results obtained by using the time resolved spectroscopy one can notice that the decrease in activity is accompanied with the shift of the transient absorption to the shorter wavelengths. The latter happens in subpicosecond time domain and was attributed to trapping of the hot and shallow trapped carriers by doping metals. This is an additional trapping channel for the hot and shallow trapped carriers, which reduces their lifetime. Therefore, the results of this study can be interpreted in favour of crucial importance of the hot and/or shallow trapped carriers for the photocatalytic activity of TiO_2 particles. This is in accordance with the previously reported results of the importance of the subpicosecond hot and/or shallow trapped hole transfer in photocatalytic oxidation of thiocyanate ion, SCN^-, on TiO_2 surface [21,25,26]. Also the accurate determination of the hot/shallow trapped carrier lifetimes was impossible in frame of this study and most probably requires the time resolution better than 100 fs.

Similar experiments were carried out with two times higher doping of the particles. However, no essential differences in transient absorption responses were observed. It seems that 0.2% doping concentration is already high enough for efficient trapping of the hot and shallow trapped carriers.

4. Conclusion

In the present study the effect of transition metal doping (Cr and/or Fe) on the transient absorption properties of TiO_2 particles has been studied. The femtosecond spectroscopic results indicate that a relatively larger amount of the trapped holes are formed in the doped samples. This can be explained by trapping of electrons by Fe and/or Cr. The photocatalytic reactor experiments revealed that the activities of the doped samples were considerably lower than the activity of the non-

doped sample. Thus, it seems that though the amount of the trapped holes increases by doping it does not enhance the activity of the samples.

References

[1] M.A. Fox, M.T. Dulay, Chem. Rev. 93 (1993) 341–357.
[2] D.F. Ollis, H. Al-Ekabi, Photocatalytic Purification and Treatment of Water and Air, Elsevier, Amsterdam, 1993.
[3] L. Linsebigler, G. Lu, J.T. Yates Jr., Chem. Rev. 95 (1995) 735–758.
[4] A. Fujishima, K. Hashimoto, T. Watanabe, TiO_2 Photocatalysis: Fundamentals and Applications, BKC Inc., Tokyo, 1999.
[5] A. Fujishima, T.N. Rao, D.A. Tryk, J. Photochem. Photobiol. C: Photochem. Rev. 1 (2000) 1–21.
[6] L. Companion, R.E. Wyatt, J. Phys. Chem. Solids 24 (1963) 1025–1028.
[7] M. Anpo, M. Takeuchi, J. Catal. 216 (2003) 505–516.
[8] M. Grätzel, R.F. Howe, J. Phys. Chem. 94 (1990) 2566–2572.
[9] X. Li, P.-L. Yue, C. Kutal, N. J. Chem. 8 (2003) 1264–1269.
[10] W. Choi, A. Termin, M.R. Hoffmann, J. Phys. Chem. 98 (1994) 13669–13679.
[11] S. Ikeda, N. Sugiyama, B. Pal, G. Marcì, L. Palmisano, H. Noguchi, K. Uosaki, B. Ohtani, Phys. Chem. Chem. Phys. 3 (2001) 267–273.
[12] A. Di Paola, S. Ikeda, G. Marcì, B. Ohtani, L. Palmisano, Int. J. Photoenergy 3 (2001) 171–176.
[13] A. Di Paola, G. Marcì, L. Palmisano, M. Schiavello, K. Uosaki, S. Ikeda, B. Ohtani, J. Phys. Chem. B 106 (2002) 637–645.
[14] A. Di Paola, E. García-López, S. Ikeda, G. Marcì, B. Ohtani, L. Palmisano, Catal. Today 75 (2002) 87–93.
[15] V. Brezová, A. Blažková, L. Karpinský, J. Grošková, B. Havlínová, V. Jorík, M. Čeppan, J. Photochem. Photobiol. A: Chem. 109 (1997) 177–183.
[16] Z. Yuan, J. Jia, L. Zhang, Mater. Chem. Phys. 73 (2002) 323–326.
[17] A. Furube, T. Asahi, H. Masuhara, H. Yamashita, M. Anpo, Chem. Phys. Lett. 336 (2001) 424–430.
[18] S. Karvinen, R.-J. Lamminmäki, Solid State Sci. 5 (2003) 1159–1161.
[19] N.V. Tkachenko, L. Rantala, A.Y. Tauber, J. Helaja, P.H. Hynninen, H. Lemmetyinen, J. Am. Chem. Soc. 121 (1999) 9378–9387.
[20] D.P. Colombo Jr., K.A. Roussel, J. Saeh, D.E. Skinner, J.J. Cavaleri, R.M. Bowmann, Chem. Phys. Lett. 232 (1995) 207–214.
[21] X. Yang, N. Tamai, Phys. Chem. Chem. Phys. 3 (2001) 3393–3398.
[22] D. Bahnemann, A. Henglein, J. Lilie, L. Spanhel, J. Phys. Chem. 88 (1984) 709–711.
[23] T. Yoshihara, R. Katoh, A. Furube, Y. Tamaki, M. Murai, K. Hara, S. Murata, H. Arakawa, M. Tachiya, J. Phys. Chem. B 108 (2004) 3817–3823.
[24] D. Dvoranová, V. Brezová, M. Mazúr, M.A. Malati, Appl. Catal. B: Environ. 108 (2002) 91–105.
[25] A. Furube, T. Asahi, H. Masuhara, H. Yamashita, M. Anpo, Res. Chem. Intermed. 27 (2001) 177–187.
[26] M. Salmi, N. Tkachenko, V. Vehmanen, R.-J. Lamminmäki, S. Karvinen, H. Lemmetyinen, J. Photochem. Photobiol. A: Chem. 163 (2004) 395–401.